Separation Science and Technology
Publication details, including instructions for authors and subscription information:
http://www.informaworld.com/smpp/title~content=t713708471

Utilization of Multivariate Calibration Methods for the Study of K Transport through Hydrophobic Liquid Membranes by Using Isomeric Anions

Alexandre M. Antunes[a]; Pedro L. O. Volpe[a]; Ronei J. Poppi[a]
[a] INSTITUTO DE QUÍMICA, UNIVERSIDADE ESTADUAL DE CAMPINAS, BRAZIL

Online publication date: 29 January 1999

To cite this Article Antunes, Alexandre M. , Volpe, Pedro L. O. and Poppi, Ronei J.(1999) 'Utilization of Multivariate Calibration Methods for the Study of K Transport through Hydrophobic Liquid Membranes by Using Isomeric Anions', Separation Science and Technology, 34: 2, 289 — 303
To link to this Article: DOI: 10.1081/SS-100100651
URL: http://dx.doi.org/10.1081/SS-100100651

SEPARATION SCIENCE AND TECHNOLOGY, **34**(2), pp. 289–303, 1999

Utilization of Multivariate Calibration Methods for the Study of K^+ Transport through Hydrophobic Liquid Membranes by Using Isomeric Anions

ALEXANDRE M. ANTUNES, PEDRO L. O. VOLPE, and RONEI J. POPPI*
INSTITUTO DE QUIMICA
UNIVERSIDADE ESTADUAL DE CAMPINAS
C. P. 6154-CAMPINAS-SP, CEP 13083–970, BRAZIL

ABSTRACT

This work describes utilization of the multivariate calibration method PLS (partial least squares) in the investigation of K^+ transport through a choloroform membrane by using mixtures of three isomeric organic anions as counterions. A comparison between the results obtained by this method and those obtained by the stepwise multiple linear regression method was also made. The BLM (bulk liquid membrane) method was employed in the transport by using a neutral crown ether, 18-crown-6 (18C6) as the carrier. Multivariate calibration was necessary since there are superpositions among the UV-Vis spectra of the three isomers. Univariate methods are shown to be unable to quantify samples in these conditions.

Key Words. Liquid membranes; Multivariate calibration; Transport of K^+

INTRODUCTION

Among several mechanisms of transport of ionic species through liquid membranes that have been demonstrated, the transport mediated by mobile carriers is one of the simplest for the removal, selective or not, of an ion

* To whom correspondence should be addressed.

from a solution (1). The transport can be made by diffusion or more actively (by using a carrier, e.g., a crown ether). When we want to establish thermodynamic properties of the transfer process, or to evaluate the potential of a new carrier, the most useful technique is the so-called ''bulk liquid membrane'' (BLM) procedure. This method is very slow, thus it cannot be used in industrial processes; a very common method in these cases is the so-called ''liquid surfactant membrane'' (LSM) process (1).

The transport of species through membranes is frequently performed with a crown-ether-type carrier using macrocyclic ligands which have a strong affinity for alkali metal cations. Each crown ether has a cavity size characteristic, estimated by the CPK (Corey–Pauling–Kolton) atomic model. According to this model, a more stable complex between the crown ether and an ionic species will be formed if the ionic radius of this species and the radius of the cavity of the carrier are similar (2–6).

When a neutral crown ether is used—as in this work—the transport mechanism is called symport, shown in Fig. 1.

Four elemental processes are involved (1):

1. At the source phase/membrane interface, a guest salt is complexed with a neutral carrier
2. The resulting lipophilic complex diffuses across the membrane
3. The release of the guest salt occurs at the membrane/receiving phase interface
4. The neutral carrier, free, diffuses back across the membrane

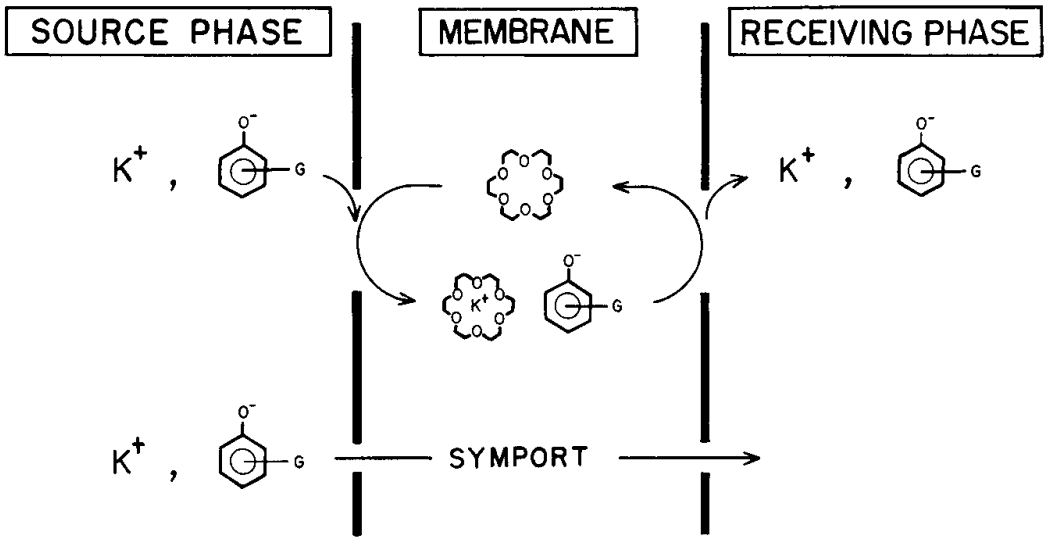

FIG. 1 Symport mechanism for cation transport.

As we observe, the anionic species is transported through the membrane together with the cation, a necessary process to maintain electrical neutrality in the bulk.

Born's equation shows that the potential energy of the transference of a species with anionic radius r and charge z from a phase of dielectric constant ϵ to another phase of dielectric constant ϵ_m, at constant temperature T, is higher as the ionic radius of this species increases (7):

$$w = z^2 e_0^2 / 8kTr\epsilon_0 \pi (1/\epsilon_m - 1/\epsilon) \quad (1)$$

where k = Boltzmann's constant, e_0 = electron charge, and ϵ_0 = electric permitivity of empty space.

The potassium ionic radius and the 18-crown-6 ether (18C6) cavity radius are very similar in size, so according to the CPK model, the formation of a 1:1 complex between cation and carrier should be observed in this case (2). In the present work, all the counterions used have the same charge (-1), so it was possible to quantify K^+ by analyzing the anion at the receiving phase by UV-Vis measurements (8), since if an anion was transported, then a K^+ was simultaneously transported (see Fig. 1).

The quantification of potassium transported into the internal aqueous phase is normally performed by a calibration curve (absorbance vs concentration). In this case this univariate method of analysis uses the absorbance measurement of a species at the wavelength in which the maxima absorbance of this species is obtained. Thus, a great part of the spectrum is discarded, and it is not possible to simultaneously study species which have similar UV-Vis spectra because spectral superposition interferes with identification and quantification.

Multivariate methods, on the other hand, make possible the study of several species undergoing transport at the same time, even if they do not have significant spectral differences or if there is a high correlation among them (9). Also, it is possible to identify baseline problems or the presence of interferents in the calibration.

In this work, the PLS (partial least squares) method (9, 10), as well as stepwise multiple linear regression (11), were used to perform our quantification.

The pioneering work in PLS was done in the late 1960s by H. Wold in the field of econometrics. The use of the PLS method for chemical applications was pioneered by the groups of S. Wold and Martens in the late 1970s after an initial application by Kowalski (10).

When the data set is a number of UV-Vis spectra, the data matrix, **X**, can be made in such a way that the spectra are put one in each line of this matrix, and the columns are the wavelengths.

A data matrix **X** can be decomposed into the sum of the product of two vectors (**t** and **p**) and a residual matrix, **E**, as shown in Eq. (2), in a procedure denoted principal component analysis (PCA):

$$\mathbf{X} = \mathbf{t}_1\mathbf{p}_1^t + \mathbf{t}_2\mathbf{p}_2^t + \cdots + \mathbf{t}_n\mathbf{p}_n^t + \mathbf{E} \quad (2)$$

Generally, PCA is made from the variance–covariance matrix, $\mathbf{X}^t\mathbf{X}$, of the spectral data (9, 10). When PCA is performed over a mean centered or autoscaled **X** and **Y** matrices, it is equivalent to performing PCA of the correlation matrix.

The first principal component is the spatial direction defined by **X** columns, which describes the maximum of variance (or dispersion) of the samples. When the total variance cannot be described with only one principal component, one can find a second component, which is orthogonal to the first, and explain the maximum of residual variance; this process continues until all the variance of the system is explained (12).

Direction coefficients of the principal component (cosines of the angles between the variables and the principal component) are called loadings, and are represented by p^t. Projection of each point on new axes gives the scores, represented by a vector **t** (one for each object or sample) (9).

Equation (2) refers to a model with *n* principal components; the **E** matrix represents that part not explained by the model, and its elements are the result of the subtraction of each element of *X* from *t*:

$$\mathbf{e}_{m,i} = \mathbf{x}_{m,i} - \mathbf{t}_m\mathbf{p}_i$$

The PLS method uses principal component modeling to represent both the independent matrix (spectra) **X** and the dependent variables matrix (concentration) **Y** by their scores, *t* and *u*, respectively. As we have seen, it is possible to write

$$\mathbf{X} = \mathbf{TP}^t + \mathbf{E} \qquad \text{and} \qquad \mathbf{Y} = \mathbf{UQ}^t + \mathbf{F}$$

where **P** and **Q** are loadings and **E** and **F** are modeling residuals for **X** and **Y**, respectively.

If we calculate the correlation between the scores of the dependent and independent variables block (*T* and *U*), we have an internal linear relationship, $U = BT$, with $B = U^tT/T^tT$ (12).

Principal components are not separately calculated for the blocks. To improve this internal linear relation between the scores, PLS makes a rotation of the axis of the principal components to produce the best relation with error reduction. This rotation removes the orthogonality of the principal components, and some authors call them latent variables instead of principal components. In this work, however, we will use principal components even for PLS.

PLS is gaining importance in many fields of chemistry. Analytical, physical, and clinical chemistries and industrial process control can benefit from the use of the method (13). More information about PLS, showing the mathematical treatment involved here and in several other methods of multivariate analysis, is presented elsewhere (9).

The SMLR (stepwise multiple linear regression) technique is based on the relationship between the concentration and absorbance values obtained at several selected wavelengths (11). The large number of absorbances available from a full spectrum makes it difficult to choose the appropriate wavelengths to be used (and their number); in fact, overfitting may provide very good calibration results of a poor predictive value. In the SMLR procedure, wavelengths are selected by first choosing that which is most highly correlated with the concentration and adding terms, one at a time, until no significantly improved standard error is obtained (13, 14). This method is a least-square approach based on the inverse of Beer's law; the concentration is modeled as a linear combination of absorbances in order to obtain the best possible correlation [$C = a_0 + a_1A_1 + a_2A_2 + \ldots$] by using a small number of wavelengths (14).

EXPERIMENTAL

In this work the isomeric anions 2,4-dinitrophenolate (2,4-DNP) and 2,5-dinitrophenolate (2,5-DNP), and also 2-hydroxybenzoate (salicylate), were employed. Some spectral differences can be observed in the UV-Vis region, although 2,4-DNP and 2,5-DNP have very similar spectra, as shown in Fig. 2.

Each spectrum corresponds to a single salt in a 1×10^{-5} mol·L^{-1} solution. It is important to note that 2,5-DNP has the highest molar absorptivity coefficient among these three, while salicylate has the smallest. A wavelength was chosen in which the maximum absorbance for each compound was found in univariate calibration studies. These wavelengths are 280, 428, and 437 nm, respectively, for salicylate, 2,4-DNP, and 2,5-DNP (8).

Univariate Method

Table 1 shows the equations for calibration curves measured for the compounds at 298 K at the maximum wavelengths, and Table 2 shows the transport rates of these three compounds, found by using the univariate method of quantification.

To compare these results with those obtained by using a multivariate model, we prepared solutions of 1, 2, and 3×10^{-5} mol·L^{-1} which were analyzed in a HP8452A UV-Vis spectrophotometer. Measured values of absorbance

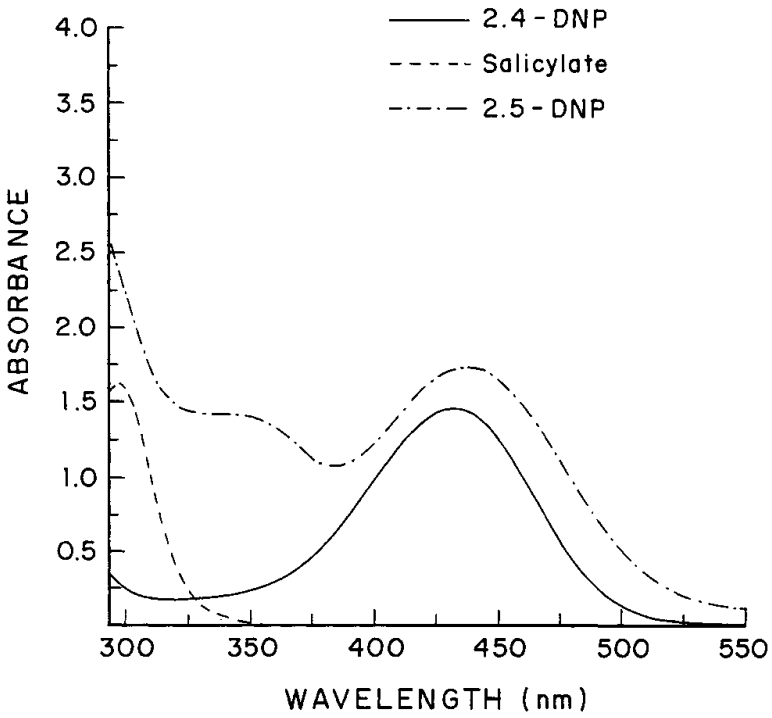

FIG. 2 2,4-DNP, 2,5-DNP, and salicylate UV-Vis spectra.

TABLE 1
Univariate Models

Compound	Model[a]	r
Salicylate	$A = 1792[C] + 0.0005$	0.9977
2,5-DNP	$A = 3350[C] - 0.004$	0.9982
2,4-DNP	$A = 7161[C] + 0.00554$	0.9995

[a] A = absorbance; C = concentration, in mol·L^{-1}.

TABLE 2
Linear Regression Obtained by Using Univariate Data

Compound	Transport rate (mol·min^{-1})
Salicylate	1.12×10^{-6}
2,4-Dinitrophenolate	1.37×10^{-6}
2,5-Dinitrophenolate	2.38×10^{-6}

MARCEL DEKKER, INC.
270 Madison Avenue, New York, New York 10016

TABLE 3
Univariate Models: Some Results

Compound	C_{real} (mol·L^{-1})	$C_{predicted}$ mol·L^{-1}	Errors (%)
Salicylate	1.0×10^{-5}	1.11×10^{-5}	11.0
	2.0×10^{-5}	2.19×10^{-5}	9.5
	3.0×10^{-5}	3.13×10^{-5}	4.3
2,5-DNP	1.0×10^{-5}	1.09×10^{-5}	9.0
	2.0×10^{-5}	2.16×10^{-5}	8.0
	3.0×10^{-5}	3.25×10^{-5}	8.3
2,4-DNP	1.0×10^{-5}	9.16×10^{-6}	−8.5
	2.0×10^{-5}	2.12×10^{-5}	5.8
	3.0×10^{-5}	3.24×10^{-5}	8.1

were put into the equations of Table 1, and new values for concentrations were found. The percent error in each case was calculated by using

$$E(\%) = [(C_{predicted} - C_{real})/C_{real}] \times 100 \quad (3)$$

Table 3 shows real and estimated values of the concentration for univariate calibration and the errors calculated with Eq. (3) for each compound.

As can be observed, the most dilute solution of salicylate has the biggest error. Since this compound has the smallest molar absorptivity coefficient (ϵ) value, the absorbances are very small. According to this, errors are smaller for 2,4-DNP, the compound with the highest ϵ.

Multivariate Method

It is important to note that real samples taken from the system had the same concentrations as the solutions used for calibration and validation of the multivariate methods.

Beginning with a 1×10^{-3} mol·L^{-1} solution, 15 mixtures were prepared containing all three compounds, with total concentrations between 8×10^{-5} and 4×10^{-4} mol·L^{-1}. Nine of these solutions were used to calibrate the method, and six were used to validate the models.

Spectra were obtained with a HP 8452A UV-Vis spectrophotometer between 190 and 820 nm, at 2 nm intervals, producing 316 variables (wavelength values), but we used only the range of wavelengths between 270 and 550 nm (141 variables).

In the experiments involving simultaneous transport of three salts, we used a U-tube system, shown in Fig. 3. As the source phase a 1×10^{-2} mol·L^{-1} mixture (pH 12) in each salt was employed. As a membrane we used a $3 \times$

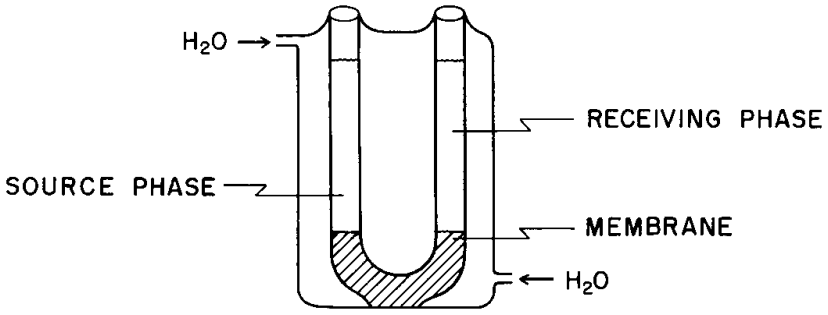

FIG. 3 U-tube used in the experiments of transport through liquid membranes.

10^{-2} mol·L^{-1} solution of 18-crown-6 in chloroform; this amount of crown ether guarantees that there was enough carrier in the membrane, thus avoiding alterations in transport rates caused by a concentration limitation of this component. Spectra of the receiving phase (distilled water at the beginning) was obtained at 5-minutes intervals. By using the PLS model we could find concentration values at each time simultaneously for salicylate, 2,4-DNP, and 2,5-DNP (PLS2 procedure), and then we constructed other curves (concentration $\times$ time) to determine the transport rates for each specie.

RESULTS AND DISCUSSION

The first step in the PLS calculations consists in finding a better number of principal components to perform the best predictions. Among the methods used to realize this procedure, cross-validation (9) is most often employed. It is the best internal validation method to find the number of principal components to model the system. Like the external validation approach, it seeks to validate the calibration model on independent test data.

In a full cross-validation process, the calibration is repeated *1* times, each time treating one *I*th part of the whole calibration set as a prediction object. In the end, all the calibration objects have been treated as prediction objects and the estimated mean square error of cross-validation (MSECV) can be computed as:

$$\text{MSECV} = (\Sigma(y - y_p)^2)/n$$

where y = actual value, y_p = predicted value, and n = number of samples.

Since full cross-validation is based on repeated calibrations which may be somewhat time-consuming for the computer, an important alternative is to perform cross-validation by splitting the calibration set into M ($M < I$) segments and then calibrating only M times, each time testing about a $1/M$ part

of the calibration set (9). In this work the calibration set was split in six segments, and then 1/6 of the calibration samples were treated as a test sample each time.

A graph of prediction errors sum of squares (PRESS) versus principal component (PC) number is shown in Fig. 4. We noted that by using four principal components, the PRESS was a minimum, so we used four principal components for this modeling.

In this study all the samples have leverage (h) in a normal range, smaller than $3K/N$ [K = number of principal components, N = number of samples (9, 10); $h = (3 \times 3)/10 = 0.9$] as shown in Fig. 5. This means that these variables are being well modeled by PLS since they have low residuals and do not have any problem of non linearity. This was expected because we are working in a low concentration range and there are no deviations from Beer's law. Leverage is a measure of the distance of a sample from the center of the data set; that is, leverage is the position of the observations of several independent variables with respect to the others.

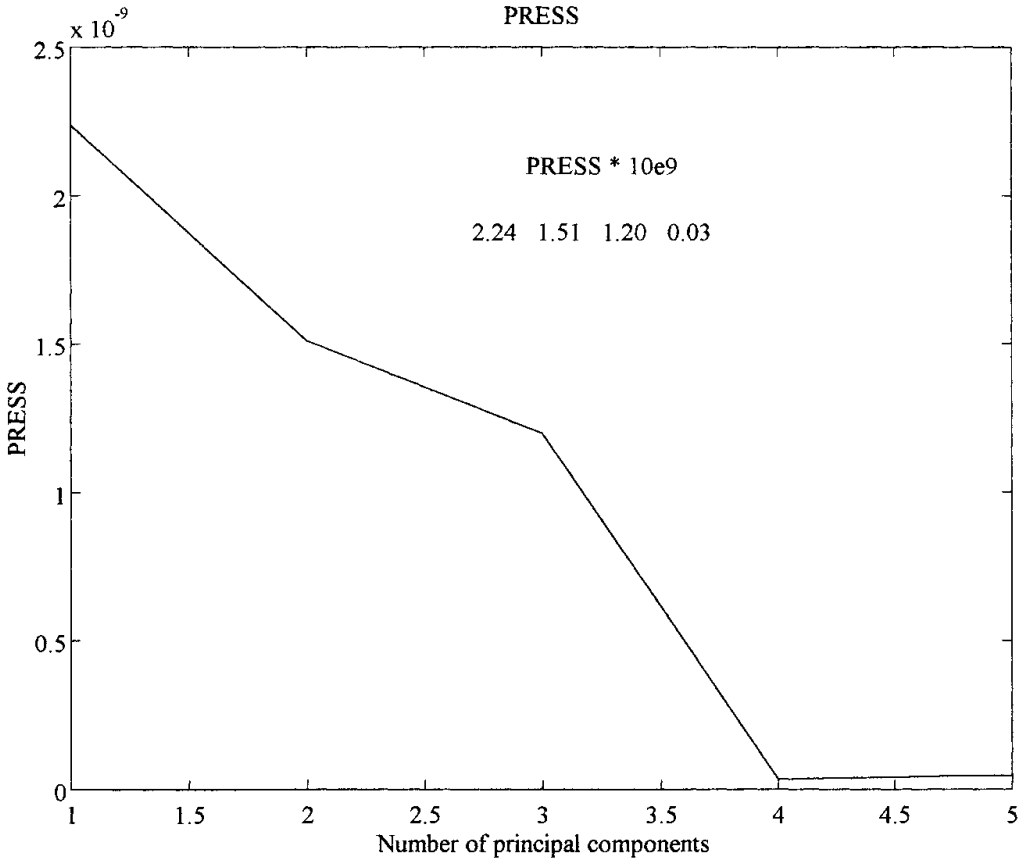

FIG. 4 PRESS vs PC number plot.

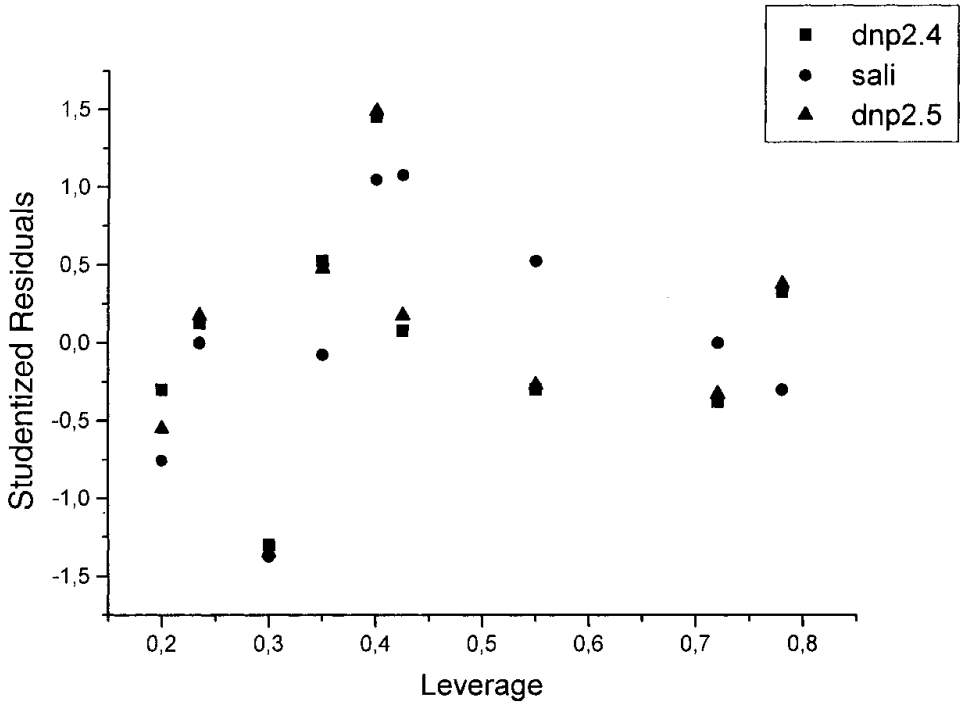

FIG. 5 Studentized residuals vs leverage plot (4 PC model).

High leverage values show that an object is far from the mean, and this fact causes an increase in the PC number calculated (an extra component was necessary to model that object). On the other hand, low values of h mean that an object is close to the mean and do not have a significant importance to the solution of the calibration.

In Fig. 5 is also possible to observe that there is some scattering in the studentized residuals, but this can be considered normal because samples with erroneous reference values (predicted variable) will tend to have a large studentized residual (>3).

The explained variance of four principal components in the PLS model is shown in Table 4. It is possible to see that with four principal components it is possible to describe 99.99% of the variance in the X-Block and 99.85% in the Y-Block.

Table 5 shows the calculated error in prediction of validation samples for each phenolic derivative by using a four-components PLS model. These error values are smaller than those found with univariate models, as expected. For salicylate there was a sample that had an error of 11.22%, probably because this sample has a salicylate concentration much smaller than the concentra-

MARCEL DEKKER, INC.
270 Madison Avenue, New York, New York 10016

TABLE 4
PLS Explained Variance (model with four principal component)

	Described variance of PLS model			
	X-Block		*Y*-Block	
PC #	This PC	Total	This PC	Total
1	83.17	83.17	52.23	52.23
2	16.22	99.38	34.63	86.86
3	0.22	99.60	11.52	98.38
4	0.39	99.99	1.48	99.85

tions of 2,4-DNP and 2,5-DNP whose molar absorptivity coefficients are significantly higher.

By using multivariate calibration we can try to identify possible abnormalities in samples of the validation set with Q and T^2 parameter values. Q is simply the sum of squares of each row (sample) from the error matrix, E (Eq. 2), and indicates how well each sample conforms to the model (14); in other words, it is a measure of the distance off the plane containing the ellipse formed by the principal components (a hyperplane if there are only two PC's). The Q limit defines a distance off the plane that is considered unusual based on the data used to form the model.

T^2 is the sum of normalized squared scores and indicates the variation in each sample within the model. We can say that T^2 is a measure of the distance

TABLE 5
Actual and Predicted Values of Validation Sample Concentrations and Calculated Percent Errors

[2,4-DNP] 10^4 M			[Salicylate] 10^4 M			[2,5-DNP] 10^4 M		
Actual	Predicted	Error (%)	Actual	Predicted	Error (%)	Actual	Predicted	Error (%)
0.1000	0.0953	−4.70	0.0800	0.0825	3.13	0.3000	0.3048	1.60
0.3000	0.2910	3.00	0.1000	0.0969	−3.10	0.0800	0.0802	0.25
0.0800	0.0772	−3.50	0.1000	0.1065	6.50	0.3000	0.3161	5.37
0.2000	0.2027	1.35	0.0900	0.1001	11.22	0.4000	0.3806	−4.85
0.2000	0.2014	0.70	0.4000	0.4036	0.90	0.0900	0.0881	−2.11
0.3000	0.2972	−0.93	0.1000	0.1046	4.60	0.2000	0.2057	2.85

TABLE 6
2,4-DNP, Salicylate, and 2,5-DNP Concentrations in the Receiving Phase during the Transport

Time (minutes)	[2,4-DNP] 10^5 mol·L^{-1}	[Salicylate] 10^5 mol·L^{-1}	[2,5-DNP] 10^5 mol·L^{-1}
0	0.0976	−0.0537	0.3982
5	0.0975	−0.0485	0.4003
10	0.0991	−0.0323	0.3997
15	0.1103	−0.0116	0.3989
20	0.1465	0.0127	0.3982
25	0.1983	0.0379	0.4051
30	0.2500	0.0621	0.4216
35	0.2854	0.0761	0.4446
40	0.3281	0.0987	0.4731
45	0.3729	0.1214	0.5087
50	0.4107	0.1415	0.5433
55	0.4493	0.1638	0.5810
60	0.4874	0.1869	0.6199
65	0.5205	0.2084	0.6551
70	0.5530	0.2316	0.6898
75	0.5859	0.2529	0.7274
80	0.6116	0.2710	0.7576
85	0.6437	0.2939	0.7954
90	0.6735	0.3151	0.8307

from the multivariate mean. The T^2 limit defines an ellipse on the plane within which the data normally projects. Adequate equations are found in the literature (14) to calculate these two parameter limits.

In this work we did not observe any abnormality in validation samples by plotting $Q \times T^2$, meaning that the modeling was satisfactory. With this model we predict each phenolic derivative concentration in the receiving phase of the bulk system employed after 90 minutes of transport. Each measure was made with 5-minutes intervals, and the results are shown in Table 6.

The same data set was used to perform SMLR calculations. For the first compound (2,4-dinitrophenolate) the variables employed were 55, 60, and 65, corresponding to 300, 310, and 320 nm. For the second compound (salicylate) the variables 20, 30, and 35 (230, 250, and 260 nm) were used. Finally, for 2,5-dinitrophenolate (third compound), six variables were necessary: 20, 30, 40, 50, 60, and 70 (230, 250, 270, 290, 310, and 330 nm).

With this methodology the results obtained were quite similar to the PLS2 results, but worse, as shown in Table 7. For the salicylate, however, the errors obtained were the largest. This was expected because it used only three

TABLE 7
SMLR Results

[2,4-DNP] 10^4 M			[Salicylate] 10^4 M			[2,5-DNP] 10^4 M		
Actual	Predicted	Error (%)	Actual	Predicted	Error (%)	Actual	Predicted	Error (%)
0.1000	0.0982	−1.80	0.0800	0.0970	21.25	0.3000	0.2706	−9.80
0.3000	0.2902	−3.27	0.1000	0.1026	2.6	0.0800	0.0651	−18.63
0.0800	0.0801	0.13	0.1000	0.1216	21.60	0.3000	0.2825	−5.83
0.2000	0.1850	−7.50	0.0900	0.1001	11.22	0.4000	0.4082	2.05
0.2000	0.2086	4.30	0.4000	0.3849	−3.78	0.0900	0.1034	14.89
0.3000	0.2919	−2.70	0.1000	0.1089	8.90	0.2000	0.2008	4.40

variables to modelate the behavior of a compound that has a small molar absorptivity. Therefore we did not calculate the transport rates based on these results because they would not be better than the PLS2-based results.

The first results, up to 15 minutes, were discarded when we calculated the slope of the concentration vs time plot which gives the transport rate of each compound. For each phenolic derivative we made a simple linear regression; the results are shown in Table 8.

We did not include the results of less than 15 minutes of transport in calculations of the slope of concentration time, which is itself the rate of transport, because the salicylate results were negatives. This occurs because the molar absorptivity of this compound is very small, as noted above, and up to 15 minutes the transported quantities are so low that the values of absorbance found are within spectrophotometer error.

If we compare these results with those found in transport experiments of only one compond at a time, we observe that in situations with more than one phenolic derivative the ratio of transport rates is smaller (Table 9), proba-

TABLE 8
Linear Regression of Table 6 Data
(rate transport calculation)

Compound	Transport rate ($mol \cdot min^{-1}$)	r
2,4-Dinitrophenolate	4.61×10^{-6}	0.99702
Salicylate	2.60×10^{-6}	0.99973
2,5-Dinitrophenolate	3.69×10^{-6}	0.98803

TABLE 9
Ratio of Transport Rates in Two Different Situations

	2,4-DNP	Salicylate	2,5-DNP
One at a time	2.13	1.00	1.22
Three at a time	1.25	1.00	1.77

bly because there are interactions between the two compounds. This occurs in this case between 2,4- and 2,5-DNP, which are the most similar compounds.

CONCLUDING REMARKS

This work shows the great potential of multivariate techniques of analysis and their ability for modeling compared to traditional methods.

A four principal component model provided very small errors in predictions for a validation set of data, and these errors were significantly smaller than those found with univariate methods.

By using the SLMR method the errors were larger than those found with PLS2. This is attributed to the influence of salicylate (molar absorptivity coefficient smaller than the isomers' coefficients).

When a mixture is being transported, we found that the variation in the ratio of transport rates among the compounds shows an inversion between 2,4- and 2,5-dinitrophenolate. Relatively, the transport of 2,4-DNP became slower and that of 2,5-DNP became faster.

REFERENCES

1. T. Araki and H. Tsukube, *Liquid Membranes*: *Chemical Applications*, CRC Press, Boca Raton, FL, 1990.
2. R. Hilgenfeld and W. Saenger, *Top. Curr. Chem.*, *101*, 3–75 (1982).
3. J. J. Christensen, D. J. Eatough, and R. M. Izatt, *Chem. Rev.*, *74*, 351 (1974).
4. C. Kappenstein, *Bull. Soc. Chim. Fr.*, *1–2*, 89–109 (1974).
5. R. M. Izatt, R. E. Terry, B. L. Haymore, L. D. Hansen, N. K. Dalley, A. G. Avondet, and J. J. Christensen, *J. Am. Chem. Soc.*, *98*, 7620–7626 (1976).
6. H. K. Frensdorff, *Ibid.*, *93*, 600–606 (1971).
7. P. Lauger, in *Membranes et Communication Intercellulaire, Les Houches, Session XXXIII*, North-Holland, Amsterdam, 1981.
8. A. M. Antunes and P. L. O. Volpe, *Quim. Nova*, *18*, 440 (1995).
9. H. Martens and T. Næs, *Multivariate Calibration*, Wiley, New York, NY, 1989.
10. M. A. Sharaff, D. L. Ilmann, and B. R. Kowalski, in *Chemometrics*, Wiley, New York, NY, 1986.

MARCEL DEKKER, INC.
270 Madison Avenue, New York, New York 10016

11. N. Draper and H. Smith, *Applied Regression Analysis*, 2nd ed., Wiley, New York, NY, 1981. S. Wold, K. Esbensen, and P. Geladi, *Chem. Int. Lab. Syst.*, *2*, 37–52 (1987).
12. R. J. Poppi, M. D. Thesis, Unicamp, 1989.
13. E. V. Thomas and D. M. Haaland, *Anal. Chem.*, *62*, 1091 (1990).
14. B. M. Wise and N. B. Gallagher, *PLS—Toolbox for Use with Matlab™*, Eigenvector Technologies, Manson, USA, 1990.

Received by editor October 23, 1997
Revision received March 1998

Request Permission or Order Reprints Instantly!